Conf-9106315--1

Submitted for publication in an ACS Symposium Series volume based on a symposium on *Colloid and Interfacial Aspects of Groundwater and Soil Cleanup* which was sponsored by the Division of Colloid and Surface Chemistry at the 65th Annual Colloid and Surface Science Symposium, Norman, OK, June 17-19, 1991. The volume is expected to be in print by April, 1992.

CONF-9106315--1

DE92 004336

THE INFLUENCE OF SURFACTANT SORPTION ON CAPILLARY PRESSURE-SATURATION RELATIONSHIPS

F.N. Desai, A.H. Demond and K.F. Hayes

Department of Civil and Environmental Engineering
The University of Michigan
Ann Arbor, MI 48109-2125

The capillary pressure-saturation relationship, a fundamental relationship in the description of multiphase flow, depends on the interfacial properties of the system. Sorption of a cationic surfactant such as cetyltrimethylammonium bromide (CTAB) at the various interfaces of a system changes interfacial properties such as electrophoretic mobility, interfacial tensions, and contact angle. The objective of this paper is to examine the effect of the changes in these interfacial properties on the capillary pressure-saturation relationships for the air-water-silica system. The results presented here show that as the sorption of CTAB increases, the naturally negatively-charged silica surface becomes positively charged. This change in charge is reflected in the contact angle which passes through a maximum when the electrophoretic mobility is close to zero. The spontaneous imbibition capillary pressure relationship is more sensitive to changes in interfacial properties than the drainage relationship. In the air-water-silica system studied here, no imbibition is observed at the maximum contact angle. The surface tension and contact angle can be used to predict both the drainage and imbibition relationships of the air-water-silica-CTAB systems from that of the air-water-silica system. The prediction is

FG02-89ER6082

accomplished through scaling using the value of surface tension and the operational contact angle, which can be obtained from the intrinsic angle through the incorporation of corrections for roughness and interfacial curvature. A comparison of the measured and calculated capillary pressure relationships shows that it is possible to predict the effect of surfactant sorption on both drainage and imbibition capillary pressure-saturation relationships for the system studied.

To describe the movement of water in the vadose zone, Richards' equation is commonly used. To apply this equation, additional information in the form of constitutive relationships must be provided. Much research has been devoted to the description and prediction of the constitutive relationship of capillary pressure-saturation (*1-3*). However, many of these efforts seem implicitly to regard the soil matrix as strongly water-wet. But that state, in reality, depends on the nature of the soil solids, the composition of the subsurface water and the properties of solutes present. If a surface-active compound is added to or naturally occurs in the subsurface, it will sorb differentially at the three interfaces of the system: air-water, water-solid and air-solid. The exact degree of sorption will be influenced by the pH and ionic strength of the aqueous solution. The sorption will, in turn, alter the interfacial tensions and the contact angle of the system, consequently impacting the capillary pressure-saturation relationships.

Since the interfacial tension between a fluid and a solid cannot be measured directly, surrogate measurements, such as electrophoretic mobility or zeta potential, are commonly used as indicators of interfacial conditions. A number of studies have related sorption or zeta potential to the magnitude of the contact angle in air-water-mineral-surfactant systems (*4-7*). These studies showed that the sorption of cationic surfactants to a negatively-charged mineral surface caused the surface charge to become positive. The increase in the surface charge resulted in the mineral surface to become first less water-wet and then strongly water-wet once again. Similar effects are also noted in organic liquid-water-mineral studies, but the range of wettability changes which result from the adsorption of surface-active compounds may be even greater (*8-9*). While in each case cited above the effects of sorption on wettability were demonstrated, the implications of these changes with respect to capillary pressure were not explored.

On the other hand, Morrow (*10-11*) and Demond and Roberts (*12*) have looked at the effects of interfacial tension and contact angle on capillary pressure-saturation relationships. Their work showed that the contact angle affects the spontaneous imbibition relationship more strongly than the primary drainage. Above a contact angle of about 65°, no spontaneous imbibition occurred. However, in these studies, the changes in contact angle and interfacial tension were accomplished through the use of different organic liquids, rather than through the sorption of a surface-active compound. Furthermore, Demond and Roberts (*12*) demonstrated a means of scaling capillary pressure-saturation relationships using the liquid-liquid interfacial tension and contact angle. Again, this methodology was developed for organic liquid-water systems and its applicability to a system where the wettability changes are governed by sorption reactions has yet to be demonstrated.

Thus, previous studies have focused on the relationship between sorption and contact angle, or on the relationship between contact angle and capillary pressure. The purpose of this paper is to integrate these foci and examine the effects of surfactant sorption on capillary pressure by correlating measurements of sorption, electrophoretic mobility, surface tension and contact angle with changes in the capillary pressure-saturation relationship for the air-water-silica system.

Background

The presence at waste disposal sites of a variety of surface-active species, such as organic acids, chelating agents, and humic substances, is not uncommon (*13*). Despite this observation, little work has been devoted to understanding the effects of sorption of these types of solutes on the movement of water in the vadose zone. Progress has been made in the numerical solution of Richards' equation (*14-15*); yet, little attention has been devoted to the changes in key constitutive properties such as the capillary pressure-saturation and relative permeability-saturation relationships that might result from the presence of surface-active contaminants. Some recent studies examine the changes in these relationships which occur due to the introduction of a separate organic liquid phase (*12, 16-18*). Nevertheless, this work is still primarily oriented towards developing models for these constitutive properties, rather than towards understanding the phenomena governing the behavior of these relationships. Ultimately, to understand the behavior of these macroscopic relationships, it is necessary to examine the microscale parameters influencing them.

Richards' equation may be written:

$$\frac{\partial \theta}{\partial t} - \nabla \cdot K \nabla P_W - \frac{\partial K}{\partial z} = 0 \qquad (1)$$

where K = unsaturated hydraulic conductivity, which may be expressed as relative permeability, k_r, where $k_r = K/K_{sat}$, and K_{sat} = saturated hydraulic conductivity,

P = pressure,

θ = moisture content of wetting phase, often expressed in terms of saturation, S, where $S = \theta/n$, and n = porosity, and

subscript W = wetting phase, usually water.

To solve this equation, additional information must be provided in the form of constitutive relationships, such as the capillary pressure-saturation relationship:

$$P_{NW} - P_W = P_c = f(S) \qquad (2)$$

where subscripts

c = capillary, and

NW = nonwetting.

in which capillary pressure, defined as the difference between the pressures in the wetting and nonwetting fluids, averaged over a representative elementary volume, is expressed as a function of saturation.

Although this relationship is macroscopic, based on a continuum approach to describing flow in porous media, it represents the effect of pore-level interfacial properties. At the scale of a single pore, the capillary pressure is described by the Young-Laplace equation:

$$P_C = \gamma_{H_2O/AIR}\,(1/R_1 + 1/R_2) \tag{3}$$

where R = principal radius of curvature,

γ = interfacial tension,

subscripts AIR = air phase, and

H_2O = aqueous phase.

If the meniscus is spherical and the pore cylindrical, then equation 3 may be rewritten as:

$$P_C = \frac{2\,\gamma_{H_2O/AIR}\cos\theta}{r} \tag{4}$$

where θ = contact angle, and

r = radius of pore.

The capillary pressure across a curved meniscus depends upon the contact angle which, according to Young's equation, is a function of the interfacial tensions of the system:

$$\gamma_{H_2O/AIR}\cos\theta = \gamma_{AIR/S} - \gamma_{H_2O/S} \tag{5}$$

where subscript

S = solid

In turn, these interfacial tensions are affected by the sorption density at the three interfaces of the system according to the Gibbs adsorption equation:

$$d\gamma = -RT\,(\sum_i \Gamma_i\, d(\ln a_i)) \tag{6}$$

where a_i = activity of species, i, in solution,

R = gas constant,

T = temperature, and

Γ_i = sorption density of species, i, at a given interface.

These equations delineate a causal relationship between sorption and the advective movement of water in the vadose zone. Thus, to understand how the presence of surface-active compounds might influence the movement of water in the vadose zone implies examining the effect of sorption on constitutive relationships such as capillary pressure-saturation.

The equations describing interfacial properties at a microscale cannot be applied directly to the macroscopic description of flow in porous media. Accurate values of the interfacial tensions of solids are difficult to obtain and surrogate measurements of surface conditions, such as electrophoretic mobility, are usually required. The contact angle defined by Young's equation for a smooth flat plate is often not the operative contact angle in a porous medium. For example, the roughness of a natural surface causes the contact angle to be hysteretic, showing an enlarged angle if advancing and a diminished angle if receding. In addition, the magnitude of the contact angle necessary to make equation 4 an equality is affected by the configuration of the pore. These factors make direct quantitative computations using the above equations difficult.

Yet with this framework in mind, methods have been developed for relating operative contact angles to intrinsic contact angles. Recent measurements of contact angles on rough surfaces and in bead packs have demonstrated that the operative contact angles show a systematic dependence on the Young's, or intrinsic, contact angle (*19-22*). Capitalizing on this work, Demond and Roberts (*12*) developed a methodology for calculating operative contact angles for drainage and imbibition in sands. They combined the curvature correction factor, Z(θ), defined by Melrose (*20*) to express the effect that the contact angle has on drainage or imbibition in terms of deviations from the capillary tube model:

$$Z(\theta) \equiv \frac{P_c\, r}{2\gamma_{H_2O/AIR}\cos\theta} \qquad (7)$$

with roughness corrections determined empirically by Morrow (*21*) (Table 1):

Table 1. Roughness Corrections for Well-Roughened Surfaces

Intrinsic Angle	Operational Angle	
	drainage (receding angle)	imbibition (advancing angle)
$0° < \theta_{INT} < 21.6°$	$\theta_r = 0°$	$\theta_r = 0°$
$21.6° < \theta_{INT} < 87.6°$	$\theta_r = 0.5\exp(0.05\theta_{INT}) - 1.5$	$\theta_r = 2(\theta_{INT} - 21.6)$

where subscripts

INT = intrinsic, and

r = corrected for roughness.

to produce a means of calculating the operational angles for both drainage and imbibition. The operational contact angles can then be combined with a form of Leverett's (*23*) equation, written here assuming that the porosity and permeability of the systems are equal,

$$P_c(S_e)_2 = P_c(S_e)_1\ (\gamma_2/\gamma_1) \tag{8}$$

where S_e = effective saturation = $(S - S_r)/(1 - S_r)$,

S_r = residual saturation of the wetting phase,

to yield:

$$P_c(S_e)_2 = P_c(S_e)_1 \frac{[\gamma \cos\theta_r\ Z(\theta)]_2}{[\gamma \cos\theta_r\ Z(\theta)]_1} \tag{9}$$

Equation 9 provides a means of calculating the capillary pressure of one fluid-fluid pair in a porous medium from the capillary pressure of another fluid-fluid pair in the same porous medium. This methodology has proven useful in organic liquid-water systems, but has yet to be applied to systems which include surface-active compounds. If equation 9 is applicable to air-water-silica-surfactant systems, then the changes in capillary pressure resulting from the sorption of surfactants can be estimated based on a knowledge of the relationship between sorption and $\gamma_{H_2O/AIR}$ and θ.

Experimental Materials and Methods

Materials. The solid quartz (SiO_2) was selected as the mineral for this study because it represents one of the most commonly occurring minerals in groundwater environments, and has surface properties representative of many aluminosilicates. The surface of quartz is composed of silanol surface functional groups which are deprotonated at all pH values normally encountered in subsurface environments, which imparts a negative charge to the quartz surface. In addition, quartz is available in many forms, such as smooth flat plates necessary for contact angle measurements and different particle sizes necessary for capillary pressure and sorption density measurements. Cetyltrimethylammonium bromide (CTAB) was selected as the surfactant for these studies, for complementary reasons. CTAB is a cationic surfactant which sorbs relatively strongly to a negatively charged surface. Consequently, it had the potential for causing well-defined changes in wettability.

Several forms of quartz were purchased and prepared for these studies. Two size fractions of particles, #40 and F-65 (U.S. Silica, Berkeley Springs, WV), were used. The #40 has a mean particle diameter of 7.3 µm and a surface area of 0.31 m^2/gm, and was used in the sorption and electrophoretic mobility studies. The F-65 has a particle size range of 106 to 425 µm and was used in the capillary pressure-saturation experiments. The particles were cleaned by washing several times with 0.1 N HCl followed by several washes with 15% hydrogen peroxide at a pH of about 4, to remove metal ions and organic matter (*24*). Smooth quartz slides were used for the contact angle measurements (Quartz Scientific, Fairport Harbor, OH); their cleaning is described in the section on contact angle measurements.

The purity of the CTAB, as purchased, was greater than 99% (Fluka Chemical, Hauppage, NY). Based on electrical conductivity measurements, the critical micelle concentration (CMC) of the CTAB was 9.5×10^{-4} M, which is in close agreement with the literature values (*25*). The CTAB was further purified by recrystallizing three times from a 4:1 mixture by volume of acetone and methanol (*26*). The radiolabelled CTAB was obtained from American Radiolabeled Chemicals (St. Louis, MO) and was used as purchased. All solvents used for cleaning were HPLC grade (Mallinckrodt Specialty Chemicals, Paris, KY). Ultrapure water was obtained by passing deionized, distilled water through Milli-Q (Millipore, Bedford, MA) cartridge filters.

Methods. To examine the relationship between sorption and capillary pressure, five types of measurements were made: sorption, electrophoretic mobility, surface tension, contact angle and capillary pressure-saturation. For the purposes of describing the experimental effort, these measurements are divided into three parts: 1) surface chemical measurements, 2) surface tension and contact angle measurements, and 3) capillary pressure-saturation measurements. Sodium chloride at a concentration of 0.01 M was used as the background electrolyte in all the experiments. The experiments were conducted at room temperature (23±2°C).

Surface Chemical Measurements. Adsorption isotherms giving adsorption density as a function of aqueous solution concentrations were measured over pH 5-9. These isotherms were obtained by mixing appropriate amounts of silica, aqueous solution containing radiolabeled CTAB, background electrolyte, and acid or base in 12 ml polypropylene centrifuge tubes, and equilibrating for over 24 hours. The slurry was centrifuged and the adsorption density calculated from the concentration of the radiotracer in the supernatant.

Potentiometric titrations were performed to give the electrophoretic mobility as a function of pH for different total CTAB concentrations. These measurements were made using a Matec ESA-8000 (Matec Applied Sciences, Hopkinton, MA). By applying an alternating electrical field to a liquid, charged particles suspended in the liquid will move electrophoretically, creating an alternating pressure wave. The signal created by such movement can be converted to electrophoretic mobility or zeta potential using the methodology developed by O'Brien (*27*).

At a particular total CTAB concentration, the silica was mixed with appropriate amounts of water, CTAB, NaCl, and acid to give a pH close to 5.5. The titration curve was obtained by incrementally adding NaOH in 0.1 pH unit aliquots and mixing for 5 mins (a time period which was sufficient to stabilize the ESA signal) after each addition. The process was repeated up to a pH of 9.5. This data was then combined with the adsorption data to give electrophoretic mobility as a function of aqueous CTAB concentration.

Surface Tension and Contact Angle Measurements. The surface tension and the contact angle on quartz of aqueous solutions of CTAB were measured for a range of CTAB concentrations at a pH of 6 and NaCl concentration of 0.01M. These measurements were made using an automated pendant/sessile drop instrument based on the Axisymmetric Drop Shape Analysis (ADSA) technique (*28*). A droplet was formed with a microsyringe (Gilmont, Great Neck, NY). The droplet was then enlarged with a M3Z Plan S microscope (Wild Leitz, Heerbrugg, Switzerland). The enlarged droplet was photographed using a solid-state CCD monochrome camera (4810 Series, Cohu, San Diego, CA), and the image sent to a digitizer where the analog signal was converted to a digital signal containing the image data in the form of pixels. A microcomputer with a 80386 microprocessor acquired these data and performed the image analysis and computation. The computational analysis involved fitting Laplace's equation to an arbitrary array of coordinate points selected from the drop profile. An objective function that expresses the deviation of the physically observed curve from the Laplacian curve was minimized to give the best value for the surface tension or contact angle (*29*). To damp vibrations, the apparatus was placed on a vibration isolation table (Technical Manufacturing, Peabody, MA).

Since the cleaning procedures influenced the reproducibility of the results, considerable attention was devoted to developing rigorous techniques. To clean the quartz slides, syringe barrels, quartz cell and other glassware, they were soaked for 20 minutes each in methanol, acetone, and Milli-Q water, followed by overnight soaking in Chromerge solution (VWR Scientific, Chicago, IL). These items were then again thoroughly rinsed in Milli-Q water. The syringe barrels and other glassware were oven dried at 110°C.

The quartz slides were not dried, but were instead stored in Milli-Q water. The stainless steel needles and teflon syringe plungers and stage were soaked for 20 minutes each in hexane, methanol, acetone, and Milli-Q water, after which the teflon parts were soaked in Micro (International Products, Trenton, NJ). After rinsing thoroughly with Milli-Q water, the teflon and steel parts were dried in the oven at 110°C.

The surface tension measurements were made by forming pendant drops of CTAB solution in air. These droplets were made using a teflon tube attached to a microsyringe adjusted with a micromanipulator (World Precision, New Haven, CT) within an environmental chamber (Rame-Hart, Mountain Lakes, NJ) which had been flushed with high purity nitrogen saturated with Milli-Q water. The surface tension dropped sharply in the first 5 minutes after the pendant drop was formed. After about 10 minutes, the surface tension became fairly constant, dropping by less than 0.3 dynes/cm every 10 minutes. Based on this, all the surface tension measurements were made at 10 minutes equilibration time.

For contact angle measurements, the quartz slide was removed from the Milli-Q water, secured to a teflon stage and placed in a quartz cell containing CTAB solution. The slide was allowed to equilibrate for 20 minutes with the CTAB solution. The needle attached to the microsyringe was passed through a teflon septum mounted on the stage and a sessile air droplet was formed on the underside of the quartz slide through a hole in the center of the slide. Both advancing and receding contact angles were measured. The measurements were made 10 minutes after the droplet was advanced or receded. After this time, the contact angle changed by less than one degree in 15 minutes.

Capillary Pressure-Saturation Measurements. The capillary pressure-saturation measurements were made using custom-made teflon-coated stainless steel pressure cells were patterned after Tempe cells (*30*). The coreholder had a height of 3.0 cm and an interior diameter of 5.5 cm. It was consistently packed with cleaned, dry F-65 silica to a consistent porosity of 0.34, in contact with a 1-bar porous ceramic plate. The cell was evacuated and then an aqueous solution (pH = 6, NaCl = 0.01 M) containing CTAB at a particular concentration was pumped through the cell at a rate of 5 ml/min until influent and effluent CTAB concentrations were the same. The CTAB concentration was measured to an accuracy of 5% by two-phase titration with mixed indicator using sodium dodecyl sulfate as the titrant

(*31*). To ensure that the system was at equilibrium, several additional pore volumes were pumped through the cell after this point.

The pressure in the aqueous phase in the cell was maintained constant, close to atmospheric pressure. The pressure in the air phase was controlled by compressed air, passed through particulate and hydrocarbon traps, regulated by two regulators in series (Model 23, Scott Specialty Gases, Plumsteadville, PA; Model 40-7, Moore Products, Spring House, PA), and monitored by a low pressure gauge (Series 66-050, Wallace and Tiernan, Belleville, NJ). The drainage relationship was measured by increasing the air pressure in small increments. After each increment in air pressure, the cell was allowed to equilibrate for at least 24 hours. The decrease in saturation within the porous medium was calculated based on the increase in weight of the bottle collecting the effluent. This procedure was repeated until a negligible efflux was achieved in response to a step increment in pressure, suggesting that residual saturation had been achieved. This point served as the beginning of spontaneous imbibition. After each small reduction in air pressure, the system was allowed to equilibrate and the increase in saturation was calculated based on the weight loss of the effluent bottle.

Results and Discussion

Surface Chemical Measurements. Figures 1 and 2 give the adsorption density and electrophoretic mobility as a function of aqueous CTAB concentration over the pH range of 6-9. Silica is negatively charged above its point of zero charge, which is in the vicinity of pH 2 (*32*). Therefore, above pH 2, a cationic surfactant such as CTAB will show strong affinity for silica, giving an isotherm shape that has been previously noted as characteristic of adsorption in these systems (*33-34*). The adsorption mechanism can be inferred from the adsorption isotherm and the electrophoretic mobility data. The adsorption isotherm can be divided into four regions (Figure 3). In region I, the adsorption is characterized by electrostatic attraction between the negatively charged surface and the positively charged head group of isolated CTAB molecules. As the negative values of the electrophoretic mobility measurements suggest, the surface does not yet have a monolayer coverage. In region II, the marked increase in adsorption is mainly due to hemimicelle formation, a result of lateral interaction between the surfactant's hydrocarbon tails. Also in this region, the electrophoretic mobility becomes increasing less negative and finally turns positive, with the isoelectric point occurring at a CTAB concentration of about 1.5 x 10^{-4} M. In region III, the slope in the isotherm decreases suggesting a lessening tendency for a positively charged surfactant to adsorb onto a increasingly positively charged surface. The adsorption which does occur in this region results primarily from the hydrophobic interaction between the hydrocarbon tails of the surfactant molecules. This strong hydrophobic interaction leads to formation of a bilayer of surfactant molecules on the surface. Finally, the adsorption isotherm reaches a plateau in region IV at an aqueous solution concentration of 5×10^{-4} M, when a complete bilayer is formed on the surface. Here, the adsorption density on the silica surface remains constant because additional molecules of surfactant introduced into the solution phase form solution-phase micelles rather than adsorbing to the solid surface.

Surface Tension and Contact Angle Measurements. Figure 4 shows the surface tension of aqueous solutions of CTAB at pH 6. The functional dependence shown in this figure is characteristic of aqueous solutions of surfactants (*35*). The surface tension decreases log-linearly from a CTAB concentration of about 1×10^{-5} M to 2.2×10^{-4} M, after which the surface tension is almost constant. These data suggest that the critical micelle concentration (CMC) of CTAB at pH 6 and NaCl = 0.01M is 2.2×10^{-4} M, which compares favorably with previously reported values (*36*).

Figure 5 shows the advancing and receding contact angles on quartz as a function of CTAB concentration at pH 6. This figure indicates that, at low CTAB concentrations of about 1×10^{-6} M, the silica surface is highly hydrophilic. A comparison of Figures 2 and 5 shows that this portion corresponds to the region where the silica is negatively charged. As the CTAB concentration increases, the contact angle increases. At an aqueous phase concentration of about 1×10^{-4} M, which is close to the isoelectric point, the advancing contact angle passes through a maximum of 64°. At concentrations close to the CMC, the contact angle decreases, suggesting that the formation of a surfactant bilayer makes the surface strongly hydrophilic again.

These observations are not unilaterally corroborated by previous investigators. For a system of air-water-quartz-CTAB (in the absence of any background electrolyte), McCaffery and Mungan (*36*) observed a maximum advancing contact angle of 60°, which occurred at a CTAB concentration of 7×10^{-4}

M, slightly below the CMC of CTAB in pure water of 9.5×10^{-4} M. In the presence of NaCl as the electrolyte, Pashley and Israelachvili (*37*) also found a maximum contact angle of about 65°. However, they believe the accurate value to be closer to 95°, attributing the lower value to impurities removable by recrystallization from a 70:30 acetone-ether mixture (*38*).

Capillary Pressure-Saturation Measurements. Figure 6 shows the drainage and imbibition capillary pressure-saturation measurements for various concentrations of CTAB at pH = 6. The imbibition relationship shows a greater range of behavior than the drainage relationship, implying a greater dependence on the surface conditions. At small contact angles, the aqueous phase imbibes strongly. As the contact angle increases, the aqueous phase imbibes less. At the isoelectric point of the CTAB-coated silica, corresponding to the maximum value of the contact angle of 64°, the aqueous phase does not imbibe. As the silica surface becomes positively charged, the contact angle decreases and the aqueous phase once again imbibes.

To determine whether these changes can be predicted on the basis of equation 9, the appropriate scaling factors were calculated (Table 2). The intrinsic angles for drainage were the receding angles given in Figure 5, whereas the intrinsic angles for imbibition were the advancing angles shown in the same figure. These angles were corrected for roughness using the equations listed in Table 1, and the suitable curvature correction factors, $Z(\theta)$, calculated according to the method outlined in Melrose (*20*). By multiplying the capillary pressures of the air-water-silica system by the calculated scaling factors, the corresponding capillary pressures for the air-water-silica-CTAB systems were estimated.

A comparison of the measured and estimated capillary pressure relationships is shown in Figure 7. This comparison demonstrates the methodology outlined here and described in more detail in Demond and Roberts (*12*) for organic liquid-water systems has the capability of predicting the effect of surfactant concentration on both drainage and imbibition capillary pressure-saturation relationships.

Table 2. Calculated Scaling Factors

Process	CTAB conc. (moles/liter)	γ (dynes/cm)	θ_{INT} (degs)	θ_r (degs)	$Z(\theta)$	Scaling factor
DRAINAGE	0.0	72	2	0	1.00	1.00
	2.5×10^{-5}	59	37	2	1.05	0.86
	1.0×10^{-4}	49	47	4	1.12	0.68
	3.0×10^{-4}	45	17	0	1.01	0.60
IMBIBITION	0.0	72	5	0	0.94	1.00
	2.5×10^{-5}	59	47	51	0.21	0.12
	1.0×10^{-4}	49	64	85	No imbibition	0.00
	3.0×10^{-4}	45	22	1	0.68	0.31

Conclusion

The results of this research show the relationship between the sorption of CTAB and capillary pressure-saturation relationships for an air-water-silica system. As CTAB sorbs to the silica surface, the silica surface becomes less negatively charged. This is reflected in the increase in the contact angle, and the corresponding decrease in spontaneous imbibition in the capillary pressure measurements. At the isoelectric point of the silica surface, the contact angle passes through a maximum of about 65°, corresponding to a total lack of imbibition. As a bilayer of surfactant molecules is formed on the silica surface, the surface becomes positively charged; the contact angle decreases, and substantial imbibition occurs again. A comparison of the measured and calculated capillary pressure relationships for these systems shows reasonable agreement, thus suggesting that the effect of surfactant sorption on capillary pressure-saturation relationships can be estimated if the surface tensions and contact angles are known. Because of the magnitude of the impact of surfactant sorption on the capillary pressure-saturation relationships, it is anticipated that the presence of surface-active contaminants in the vadose zone will have a significant effect on the advective movement of water and its dissolved constituents.

Acknowledgments

We gratefully acknowledge the support of Dr. Frank J. Wobber, Program Manager, Subsurface Science Program, Office of Health and Environmental Research, U.S. Department of Energy (Grant DOE-FG02-89-ER60820) for this research. In addition, we thank Haza Hammad for his contributions to the surface chemical measurements, Linda Timmer Verhulst for the surface tension and contact angle measurements, and Benjamin Witherell for the capillary pressure-saturation measurements.

Literature Cited

1) Arya, L.M.; Paris, J.F. *Soil Science Society of America Journal* **1981**, *45*, 1023-1030.

2) Haverkamp, R.; Parlange, J.Y. *Soil Science* **1986**, *142(6)*, 325-339.

3) Luckner, L.; van Genuchten, M.; Nielsen, D.R. *Water Resources Research* **1989**, *25(10)*, 2187-2194.

4) Ginn, M.E. In *Cationic Surfactants*, Jungermann, E., Ed., Surfactant Science Series, Marcel Dekker, NY, 1970, Vol. 4, 341-367.

5) Aronson, M.P.; Princen, H.M. *Colloid and Polymer Science* **1978**, *256*, 140-149.

6) McGuiggan, P.M.; Pashley, R.M. *Colloids and Surfaces* **1987**, *27*, 277-287.

7) Fuerstenau, D.W.; Herrera-Urbina, R. In *Cationic Surfactants*, Rubingh, D.N. and Holland, P.M., Eds., Surfactant Science Series, Marcel Dekker, NY, Vol. 37, 407-447.

8) Buckley, J.S.; Takamura, K.; Morrow, N.R. *SPE Reservoir Engineering* **1989**, *4(3)*, 332-340.

9) Gaudin, A.M.; Decker, T.G. *Journal of Colloid and Interface Science* **1967**, *24*, 151-158.

10) Morrow, N. R. *Journal of Canadian Petroleum Technology* **1976**, *15(4)*, 49-69.

11) Morrow, R.N.; McCaffery, F.G. In *Wetting, Spreading, and Adhesion*, Padday, J.F., Ed., Academic Press, New York, 1981, 387-411.

12) Demond, A.H.; Roberts, P.V. *Water Resources Research* **1991**, *27(3)*, 423-437.

13) U.S. Department of Energy. In *Subsurface Science Program: Program Overview and Research Abstracts FY 1989 - FY 1990*, U.S. Department of Energy Report No. DOE/ER-0432, Office of Energy Research, Office of Health and Environmental Research,Washington D.C., 1990, 5.

14) Milly, P.C.D. *Transport in Porous Media* **1988**, *3*, 491-514.

15) Celia, M.A.; Bouloutas, E.T.; Zarba, R.L. *Water Resources Research* **1990**, *26*, 1483-1496.

16) Lenhard, R.J.; Parker, J.C. *Journal of Contaminant Hydrology* **1987**, *1*, 407-424.

17) Lenhard, R.J.; Parker, J.C. *Water Resources Research* **1987**, *23(12)*, 2197-2206.

18) Demond, A.H.; Roberts, P.V. *Water Resources Research* **1991**, submitted for publication.

19) Shephard, J.W.; Bartell. F.E. *Journal of Physical Chemistry* **1953**, *57*, 458-463.

20) Melrose, J.C. *Society of Petroleum Engineers Journal* **1965**, *5*, 259-271.

21) Morrow, N.R. *Journal of Canadian Petroleum Technology* **1975**, *14(4)*, 42-53.

22) Zografi, G.; Johnson, B.A. *International Journal of Pharmaceutics* **1984**, *22*, 159-176.

23) Leverett, M.C. *Transactions of AIME* **1941**, *142*, 152-169.

24) Kunze, G.W.; Dixon, J.B. In *Methods of Soil Analysis, Part 1: Physical and Mineralogical Methods*, Klute, A., Ed.; American Society of Agronomy: Madison, WI, 1986, 95.

25) Mukerjee, P.; Mysels, K.J. *Critical Micelle Concentrations of Aqueous Surfactant Solutions*; National Standards Reference Data; National Bureau of Standards: Washington, DC, 1971.

26) MacRitchie, F. *Chemistry at Interfaces*; Academic Press: San Diego, CA, 1990.

27) O'Brien, R.W. *Journal of Fluid Mechanics* **1988**, *190*, 71-86.

28) Cheng, P.; Li, D.; Boruvka, L.; Rotenberg, Y.; Neumann, A.W. *Colloids and Surfaces* **1990**, *43*, 151-67.

29) Rotenberg, L.; Boruvka, L.; Neumann, A.W. *Journal of Colloid and Interface Science* **1983**, *93(1)*, 169-83.

30) Reginato, R.J.; van Bavel, C.H.M. *Soil Science Society of America Proceedings* **1962**, *26(1)*, 1-3.

31) Rosen, M.J.; Goldsmith, H.A. *Systematic Analysis of Surface-active Agents*; Wiley Interscience: New York, NY, 1972; 427-29.

32) Parks, G.A. *Chemical Reviews* **1965**, *65*, 177-198.

33) Bijsterbosch, B.H. *Journal of Colloid and Interface Science* **1974**, *47(1)*, 186-98.

34) Stratton-Crawley, R.; Shergold, H.L. *Colloids and Surfaces* **1981**, *2*, 145-54.

35) Rosen, M.J. *Surfactants and Interfacial Phenomena*; John Wiley: New York, 1989.

36) McCaffery, F.G.; Mungan, N. *Journal of Canadian Petroleum Technology* **1970**, *9(3)*, 185-96.

37) Pashley, R.M.; Israelachvili, J.N. *Colloids and Surfaces* **1981**, *2*, 169-187.

38) Pashley, R.M.; McGuiggan, P.M.; Horn, R.G.; Ninham, B.W. *Journal of Colloid and Interface Science* **1988**, *126(2)*, 569-78.

Figure 1: Adsorption of CTAB on silica as function of pH.

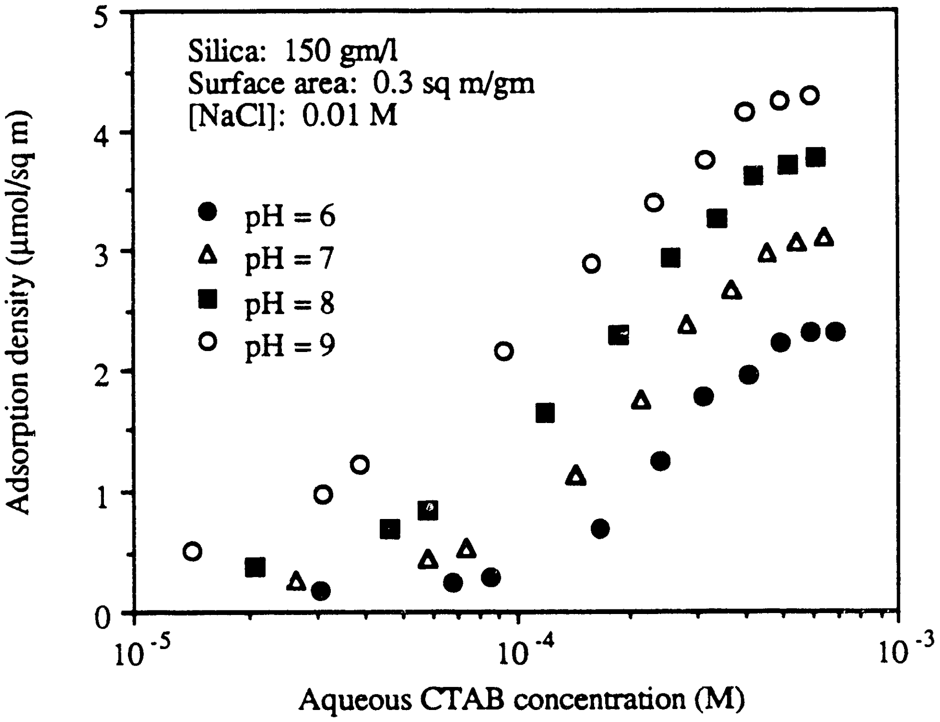

Figure 2: Electrophoretic mobility of CTAB-coated silica as a function of pH.

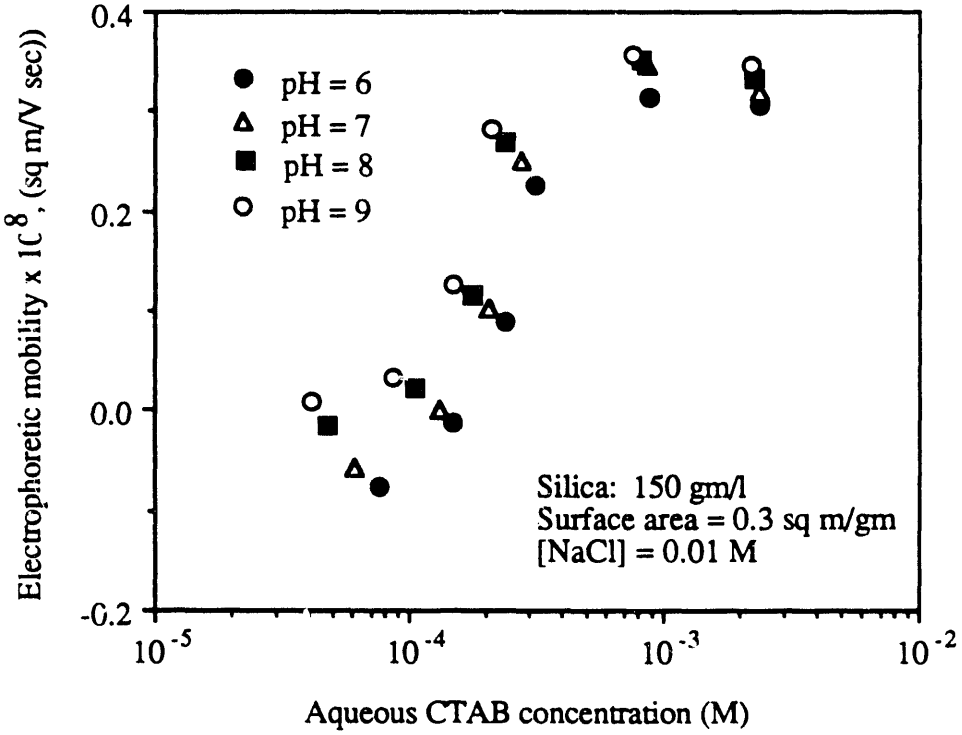

Figure 3: Adsorption density and electrophoretic mobility for CTAB on silica.

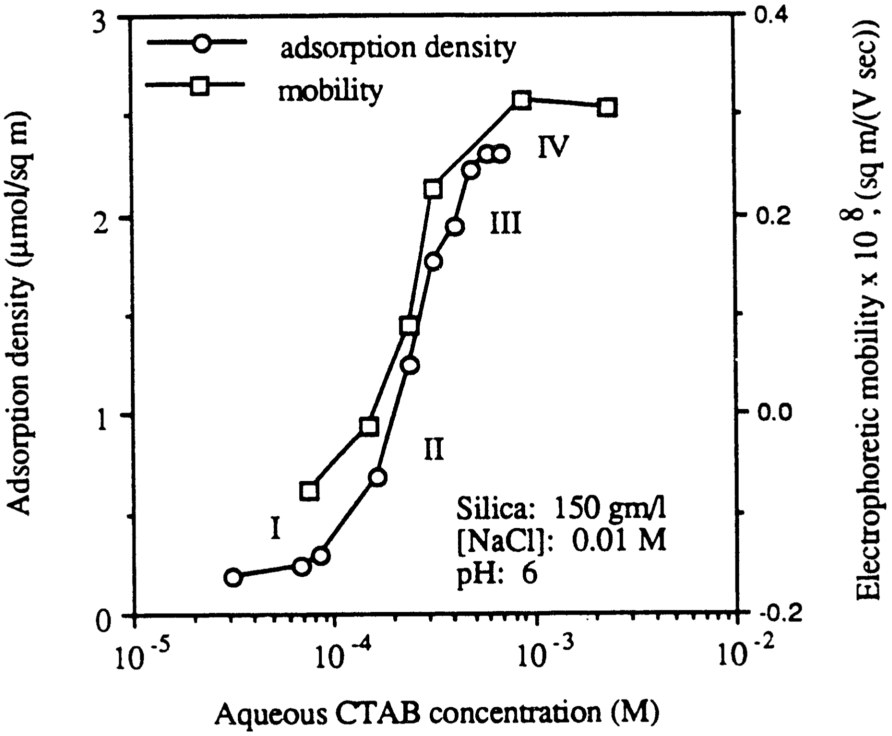

Figure 4: Surface tension of water as a function of CTAB concentration.

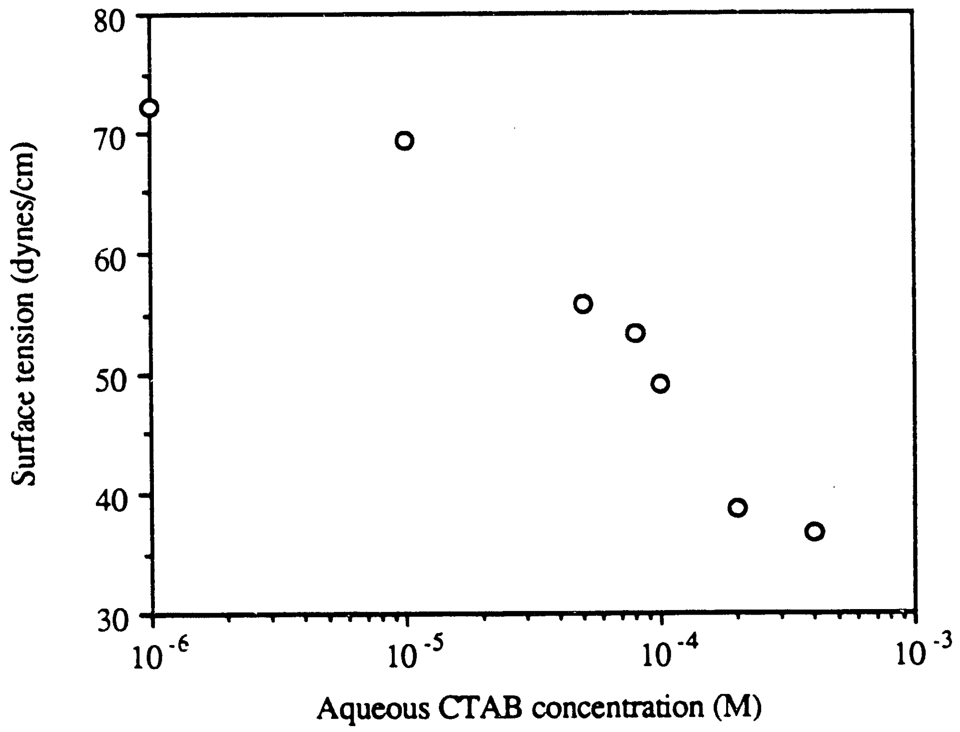

Figure 5: **Advancing and receding contact angle of water as function of CTAB concentration.**

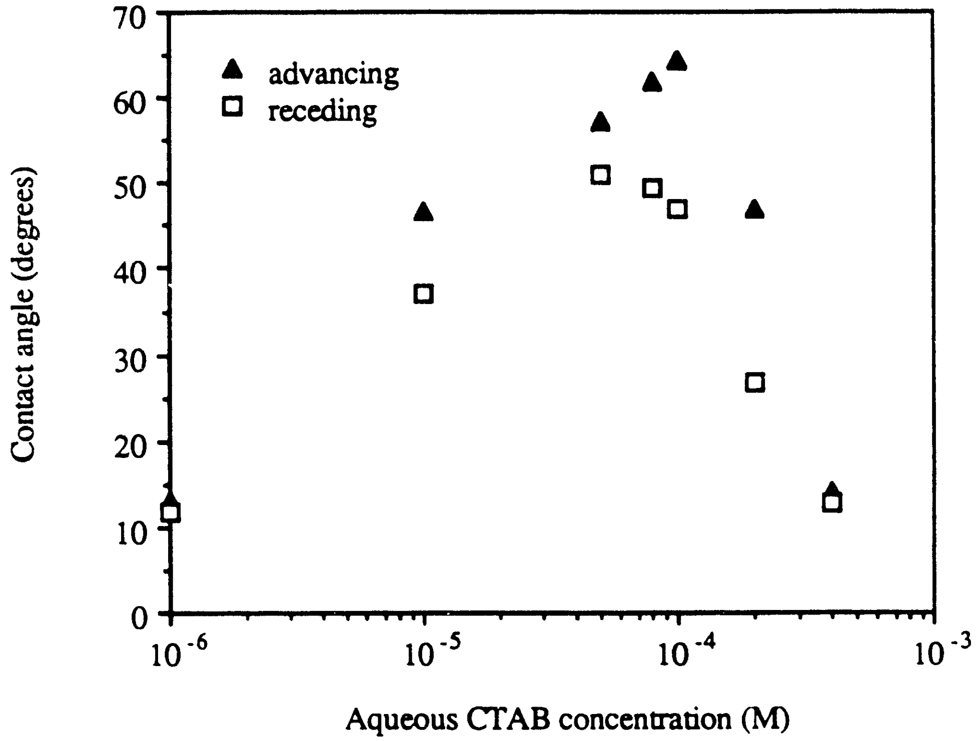

Figure 6. Drainage and imbibition capillary pressure-saturation relationships at various CTAB concentrations.

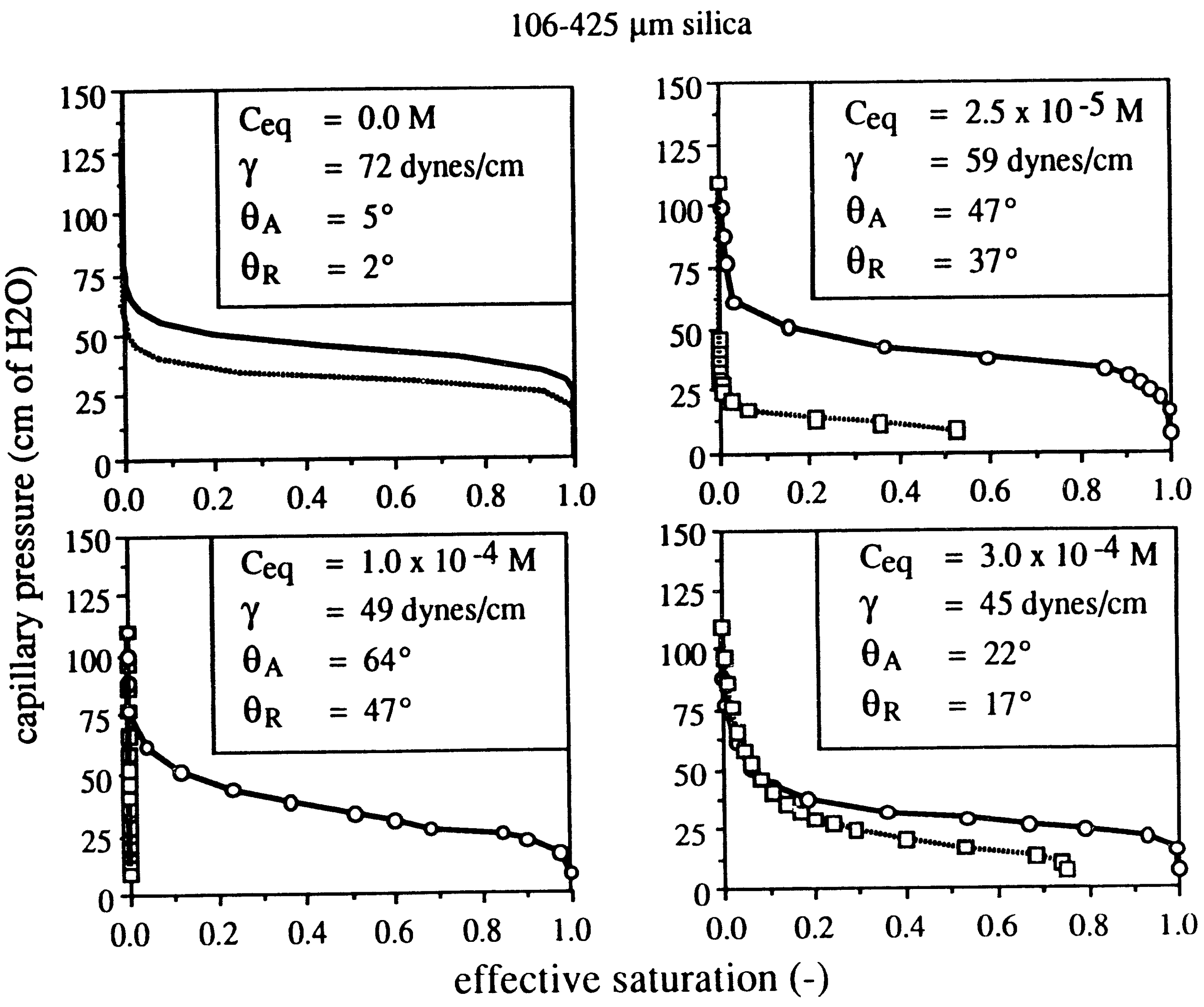

Figure 7. Comparison of measured and predicted capillary pressure-saturation relationships.

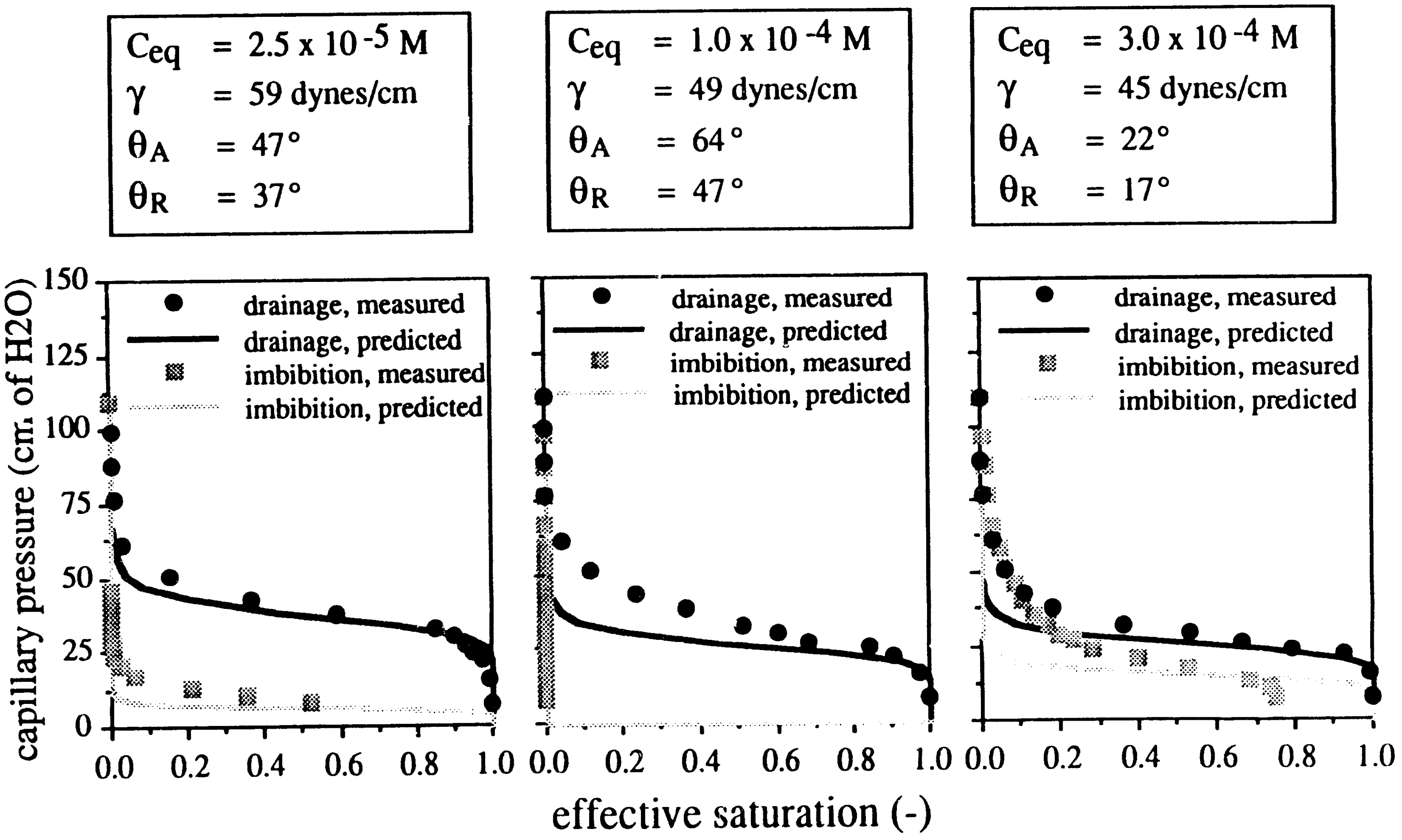

DATE FILMED

2 /03/ 92